Identification of candidate genes associated with skin yellowness in yellow chickens

Shizi He,[*,†] Tuanhui Ren,[*,†] Wujian Lin ●,[*,†] Xiuxian Yang,[*,†] Tianqi Hao,[*,†] Guoxi Zhao,[*,†] Wen Luo,[*,†] Qinghua Nie,[*,†] and Xiquan Zhang[*,†,1]

[*]Department of Animal Genetics, Breeding and Reproduction, College of Animal Science, South China Agricultural University, Guangzhou, 510642, Guangdong, China; and [†]Guangdong Provincial Key Lab of Agro-Animal Genomics and Molecular Breeding, and Key Laboratory of Chicken Genetics, Breeding and Reproduction, Ministry of Agriculture and Rural Affairs, Guangzhou, 510642, Guangdong, China

ABSTRACT The yellow color of the skin is an important economic trait for yellow chickens. Low and non-uniform skin yellowness would reduce economic efficiency. However, the regulatory mechanism of chicken skin yellowness has not been fully elucidated. In this study, we evaluated the skin yellowness of 819 chickens by colorimeter and digital camera, which are from the same batch and the same age of 2 pure lines with significant differences in skin yellowness. A total of 982 candidate differential expressed genes (**DEGs**) were detected in duodenal tissue by RNA-seq analysis for high and low yellowness chickens. Among the DEGs, we chose fatty acid translocase (**CD36**) gene and identified a single nucleotide polymorphism (**SNP**) upstream of the CD36 gene that was significantly associated with skin yellowness at multiple parts of the chicken, and its different genotypes had significant effects on the promoter activity of the CD36 gene. These findings will help to further elucidate the molecular mechanism of chicken skin yellowness and is helpful for improving chicken skin yellowness.

Key words: chicken, skin yellowness, transcriptome, CD36, SNP

INTRODUCTION

With the promotion of chilled sales, chickens with better carcass appearance are more likely to be preferred by consumers, and consumers in southern China prefer to purchase chickens with an overall yellowish skin. Bright yellow skin is usually associated with healthy and good quality flesh (Langi et al., 2018). Exploring and searching for candidate associated variants and genes for chicken skin yellowness will help to improve the yellowness of chicken skin and thus meet consumer demand.

The yellow color of chicken skin is mainly due to carotenoid deposition, and candidate genes for carotenoid coloration in birds include BCO2 (Eriksson et al., 2008), BCMO1 (von Lintig and Vogt 2000), SCARB1 (During et al., 2008), CD36 (Krieger 1999), StAR1 (Soccio and Breslow 2003; Tabunoki et al., 2004), PLIN

(Londos et al., 1996), GSTA2 (Bhosale et al., 2004). Chickens obtain carotenoids by ingesting feed, the carotenoids released from the food matrix are dissolved in fat, and the secretion of intestinal lipase, bile salts and phospholipids digest the lipid droplets and form mixed carotenoid micelles (Budny 2015). SCARB1 (Tourkova et al., 2020) and CD36 (van Bennekum et al., 2005; Sakudoh et al., 2010; Borel et al., 2013) are key participants in the recognition of mixed carotenoid micelles for transport into cells.

The carotenoids are then transported to the tissues for functioning or deposition in the tissues, during which time they may be cleaved by BCMO1 and BCO2 to form precursors of vitamin A and other metabolites. BCO2 breaks down the colorcolored carotenoids into colorless carotenoids, thus preventing the deposition of colored carotenoids in the tissues (Vage and Boman 2010; Tuzcu et al., 2017). Previous studies on chicken skin yellowness have focused more on BCO2, which may distinguish between white-skinned and yellow-skinned chickens but may have difficulty explaining differences in skin yellowness.

In birds, the duodenum and jejunum are the key sites for carotenoid absorption (Tyczkowski and Hamilton

1986). Studies showed high concentrations of lutein and carotenoids in the duodenum and jejunum (Littlefield et al., 1972; Phelan et al., 2018). Although the carotenoid content of the duodenum and jejunum is similar in chicken, the mucosal extracts of the duodenum are more lipid soluble than those of the jejunum and ileum (McLean et al., 2005). There are more phospholipids, sterols, apolipoprotein, and carotenoids packed together in the duodenum to form portomicrons (Phan and Tso 2001), which means that carotenoids are more likely to be absorbed in the duodenum. Therefore we selected the duodenum, which has a higher carotenoid absorption potential, as the subject of our study. Whereas intestinal absorption of carotenoids is a prerequisite for pigmentation in the skin, differences in chicken skin yellowness are more likely to be related to differences in the efficiency of intestinal absorption of carotenoids.

In this study, we analyzed differences in skin yellowness between 2 purebred chickens, and duodenal tissues from chickens with high and low skin yellowness were analyzed by RNA-seq to reveal candidate genes that affect skin yellowness in chickens. We identified candidate genes and metabolic pathways associated with chicken skin yellowness and identified an SNP associated with chicken skin yellowness. All these findings will likely help to unravel the molecular mechanisms of chicken skin yellowness.

MATERIALS AND METHODS

Ethics Statement

G-line and M-line chickens were obtained from Guangzhou KwangFeng Breeding Farm (Guangzhou, Guangdong Province, China). Animal experiments were conducted in accordance with the regulations and guidelines established by the Animal Care Committee of South China Agricultural University (approval number: SCAU#0106; 25 November 2018).

Experimental Population

The experimental animals were 2 pure lines of chickens from the KwangFeng Breeding Farm. In Line G yellow feather chickens, 356 females and 160 males from the same batch, and in Line M partridge chickens, 184 females and 119 males from the same batch, a total of 819 chickens, were caged under uniform rearing conditions, with free access to water and food and reasonable light during breeding. The 819 chickens were subjected to slaughtering experimental chicken traits. The chickens were all 73 d of age. All chickens were slaughtered in a slaughterhouse by bleeding through the jugular vein, then scalded in water at 64°C for 220 s and plucked with a chicken hair plucker.

Skin Color Measurements

Skin yellowness was determined using a 3nh-nh310 colorimeter (3nh, Guangzhou, China). The colorimeter gives an a* value (for red to green), a b* value (for yellow to blue) and an L* value (for brightness) directly from a single measurement. Skin yellowness is measured by the b * value. We measured the skin on the left side of the chicken on the chest, back, shoulder, and leg, averaging 3 times for each position and rotated by 90° each time. Measurements were taken to avoid areas of bruising, bleeding, discoloration and damage. Digital photographs of 819 slaughtered chickens were successfully obtained with a Canon Eos 80d color camera (Canon, Tokyo, Japan) in a small studio with a fixed light source (Travor LED Mini Photography, Hangzhou, China), with fixed camera exposure parameters (aperture value f/4.5, ISO-250, exposure time 1/400s) and with experienced workers according to the colorimetric umbrella for chicken carcasses Sensory scoring of yellowness (1 to 4 points).

We have programmed a script in python 3.6.3 to automatically extract the color values of the chicken skin. The original image was first scaled to a small size (400*267) and then the rgb values were converted to hsv space using a standard formula implemented by the CV2 package cv2.cvtColor function (Figure S1). In the hsv model, **H** denotes hue (h denotes variation in color type), **S** denotes saturation (s denotes the purity or intensity of a color) and **V** denotes luminance or brightness. The background and the chicken in the picture are distinguished according to the range of h, s and v, and the h, s and v values of the pixel points belonging to the chicken in the picture are averaged separately to obtain the h, s and v values of the chicken. A photograph is provided in Figure S2 as an example. The script "get_skin_hsv.py" is provided in the Supplementary Material.

Genetic Parameter Estimates

The restricted maximum likelihood method implemented by the DMU package was used to obtain estimates of the phenotypic and genetic (co)variance and heritability, and the following linear model was used for the analysis of the data:

$$y = Xb + Za + e$$

where y was the phenotypic value of a trait, a was the vector of the animal additive genetic effect, b was the vector of the fixed effects, including gender (2 levels) and pen (90 levels in G line, 62 levels in M line), e was the vector of random residuals, and X and Z were the incidence matrices. A total of 512 individuals in G line and 351 individuals in M line with complete pedigree and phenotypic trait records were included.

DNA and RNA Extraction

Genomic DNA was extracted from blood according to the Blood DNA kit (Magen, Guangzhou, China) instructions steps, and use a Nanodrop 2000c spectrophotometer (Thermo Scientific, Waltham, MA) to measure DNA sample concentrations and then the samples were

diluted to 80 ng/μL and stored at $-20°$C for storage. Total RNA was isolated from duodenum tissues of chickens using HiPure Unviersal RNA Mini Kit (Magen).

CD36 Fragment Amplification

Full length fragment of *CD36* was loaded on NCBI (https://www.ncbi.nlm.nih.gov, accessed on 10 March 2022), and then used NCBI Primer-BLAST (Primer designing tool (https://www.ncbi.nlm.nih.gov/tools/primer-blast/) to design PCR amplification primers. The total volume of PCR was 30 μL, and the amplification system was 3 μL chicken DNA at a concentration of 100 to 200 ng/μL; 1.2 μL upstream primer (Tsingke Biotech, Beijing, China) at a concentration of 10 nM; 1.2 μL downstream primer at a concentration of 10 nM; 9.6 μL double distilled water; 15 μL Green TaqMix (Vazyme, Nanjing, China). The primer sequences are shown in Table S1. The PCR program was predenatured for the first 5 min, denatured at 95°C for 15 s, followed by annealing at 58°C for 30 s, extension at 72°C for 50 s (32 cycles), and final extension at 72°C for 5 min at the end of the cycle. It was stored temporarily at 4°C until off the machine. Then, the amplified samples were sent to Tsingke Biotech Co., Ltd. for sequencing.

RNA-seq and Bioinformatics Analysis

In Lines G and M, 3 chickens with high yellowness of chest skin were selected as high yellowness group H and three chickens with low yellowness of chest skin were selected as low yellowness group L. There was a significant difference in mean yellowness between groups H and L (11.93 $\pm$ 2.87 vs. 6.55 $\pm$ 0.88, $P < 0.001$, n = 3, sex = female). Duodenal tissue was collected after the contents of the intestine had been cleared and rapidly frozen in liquid nitrogen for RNA-Seq. RNA was extracted using TRIzol Reagent (Ambion/Invitrogen, Carlsbad, CA) and then accurately tested for RNA integrity by Agilent 2100 bioanalyzer. Enrichment of mRNA with polyA tails by Oligo (dT) magnetic beads. Library acquisition using the NEBNext Ultra RNA Library Prep Kit for Illumina, the library preparations were sequenced on an Illumina Novaseq platform and 150 bp paired-end reads were generated. We removed reads with adapters, removed N-containing reads and low-quality reads (reads with Qphred <= 20 that had more than 50% of the entire read length in bases). Paired-end clean reads were compared to the reference genome using HISAT2 v2.0.5. Feature Counts (1.5.0-p3) was used to calculate the number of reads mapped to each gene. The FPKM for each gene was then calculated based on the length of the gene and the number of reads mapped to that gene was calculated. Differential expression analysis between the 2 comparative combinations was performed using DESeq2 software (1.20.0). The method of Benjamini and Hochberg was used to adjust the resulting *P*-value to control for false discovery rates. Genes with adjusted *P*-value <= 0.05 were found to be assigned as differentially expressed by

DESeq2. We used clusterProfiler (3.8.1) software to analyse the statistical enrichment of differentially expressed genes in the KEGG pathway, and we used a native version of the GSEA analysis tool (http://www.broadinstitute.org/gsea/index.jsp) to perform separate GO, KEGG data for this species GSEA analysis.

RT-qPCR Validation of Candidate Genes

Reverse transcription was performed using a cDNA reverse transcription kit (Vazyme, Nanjing, China) according to the manufacturer's protocol. All primers (Table S1) were designed using the Primer Premier 5.0 software (Premier Biosoft, Palo Alto, Ca, United States). qPCR procedures were performed in the Quant-Stuido 5 Real-Time Detection System (Thermo Scientific, Waltham) and the ChamQ Universal SYBR qPCR Master Mix (Vazyme). Gene expression was detected using the 2-$\Delta\Delta$ct method with *GAPDH* as the reference gene.

Cell Line Culture and Transfection

Chicken hepatoma cells (**LMH**) was obtained from Hfwanwu (Hfwanwu, Hefei, China), and none of the cell lines were contaminated during the experiments. LMH cells were treated with Williams E (Procell, Wuhan, China) containing 10% fetal bovine serum (Gibco, Auckland, New Zealand) and 1% penicillin/streptomycin (Gibco) were treated and incubated at 37°Cand 5% CO_2. Transfection was performed using transfection reagents according to the instructions (Life-iLab, Shanghai, China).

Luciferase Assay

Using primer *CD36*-PGL (Table S1) to amplify the fragment containing CC and GG genotypes of SNP, PGL3-basic plasmid (Miaoling, Wuhan, China) was digested by XhoI and HindIII (Best Enzymes, Jiangsu, China), ligated overnight at 16°C by T4 ligase (Best Enzymes), and the monoclonal colony was screened for sanger sequencing to verify the successful vector construction (Supplementary Material PGL3-seq). LMH cells were inoculated into 96-well plates at a density of 1.5×10^4 cells per well. Subsequently, PGL-CC, PGL-GG, and PGL-Basic were transfected into the cells in 8 replicates per group. 48 h later, a dual luciferase reporter assay was performed according to the manufacturer's instructions (E2920, Promega; Madison, WI).

Statistical Analyses

Descriptive statistical analyses of data recorded for phenotypic traits were performed using SPSS 22.0 (SPSS Inc., Chicago, IL). Pearson's correlation coefficient (r) and linear regression were used to evaluate correlations between traits. Factor analyses were performed with eigenvalues greater than 1, and principal components

were extracted through the correlation matrix. P-value < 0.05 were considered statistically significant. For the statistical analysis of the 2 comparisons, we used the t test. We considered $P < 0.05$ to be statistically significant ($* P < 0.05$; $* * P < 0.01$; $*** P < 0.001$).

The sequence peak map files returned from sequencing were placed into Seqman in DNAStar Lasergene software (DNAStar, Madison, WI) for comparison with reference sequences, and the genotype of each SNP was recorded. A mixed linear model was used to analyze the association between SNPs and skin yellowness traits. The mixed linear model used was as follows:

$$Y = \mu + G + S + L + e$$

Y: phenotypic values for skin yellowness trait, μ: the overall mean, G: the fixed effect of genotype, S: the fixed effect of gender (2 levels), L: the fixed effect of line (2 levels), e: random residuals. Corrections for multiple comparisons were performed using the Bonferroni method (Ren et al., 2019). When 2 lines were analyzed separately, the fixed effects of line will not be included. The percentage of phenotypic variance explained (**PVE**) is calculated using GAPIT (https://www.maizegenetics.net/gapit), and PVE is equal to Rsquare.of.Model.with.SNP minus Rsquare.of.Model.without.SNP.

RESULTS

Differences of Skin Yellowness Between Line G and Line M Chickens

To understand the differences in skin yellowness between Lines G and M chickens, we evaluated 4 representative body parts using a colorimeter, and the distribution of yellowness values at each location is shown in Table 1, with the coefficient of variation shown in Table S2. Results showed that the yellowness of the skin of M-line chickens is generally higher than that of G-line chickens, that there are significant differences in skin color between G-and M-line roosters and hens, and that the coefficients of variation for the skin on the chest and back of G-line chickens are greater than those for M. In order to better understand the differences in skin color between Lines G and M, the data were downscaled by PCA analysis and the individual loadings are shown in Figure 1A. The individuals of Line G were more discrete, indicating a lower degree of uniformity between individuals, whereas males and females of Line M were more concentrated, indicating that the uniformity of skin color yellowing was higher in Line M than in Line G,

which is consistent with the results in Table S2. In order to more accurately assess the yellowness of chicken skin color, we used python(3.6.3) software to analyze the photographs to assess the overall skin color of the chickens, compensating for the fact that the colorimeter does not reflect the whole in its local measurements. The results showed significant differences in the overall skin tone of chickens between Lines G and M, with a high degree of variation between individuals. PCA analysis (Figure 1B) revealed that the b* values, photo Saturation and sensory scores were relatively close to each other at each site, suggesting that photo Saturation may be a candidate for assessing chicken skin yellowness. In summary, chicken skin yellowness and its uniformity were influenced by breed and sex, with Line M chickens having higher skin yellowness overall than Line G chickens.

Estimation of Genetic Parameters for Skin Yellowness Trait

To develop a suitable selection strategy, we evaluated the genetic parameters of traits related to chicken skin yellowness (Table 2). The heritability of skin yellowness traits was higher in Line G than in Line M, with higher heritability for breast b* value, H value and S value, and lower heritability for back and shoulder b* value. Selection for breast b* value or H value and S value of photos might achieve better effect.

Differential Expressed Genes Between Line G and Line M Chickens

To investigate the mechanism of genetic regulation of skin yellowness in chickens, we selected 3 chickens in each of Lines G and M with significant differences in skin yellowness, divided them into high yellowness (**H**) and low yellowness (**L**) groups (Figure 2A), and RNA-sequenced their duodenal tissues. The mean clean reads for H and L were 40,908,808 and 40,415,443, respectively. A PCA analysis of each sample's FPKM was performed and a trend toward separation of samples between the 2 groups was found (Figure 2B). Based on the criteria of |log2FoldChange| > 0 and P-value < 0.05, 982 differentially expressed genes were identified between H and L (Figure 2C), of which there were 351 upregulated genes and 631 downregulated genes. Based on the results of the analysis of differentially expressed genes, a clustering heat map using R software revealed

Table 1. Mean and standard error of skin yellowness traits in Lines G and M of chickens (Mean ± SEM).

	Chest b*[1]	Back b*[1]	Shoulder b*[1]	Leg b*[1]	H[1]	S[1]	V[1]	Sensory score[1]
G♀(356)[2]	10.15 ± 2.86[c]	10.96 ± 3.07[c]	11.09 ± 2.57[b]	7.23 ± 4.07[b]	53.93 ± 20.11[b]	56.44 ± 8.37[c]	184.25 ± 6.38[c]	2.51 ± 0.89[c]
G♂(160)[2]	6.19 ± 1.68[d]	6.64 ± 2.33[d]	7.78 ± 1.86[c]	2.9 ± 1.95[c]	71.24 ± 14.91[a]	51.28 ± 3.96[d]	179.66 ± 7.5[d]	1.78 ± 0.65[d]
M♀(184)[2]	12.15 ± 1.87[a]	15.11 ± 3.39[a]	13.79 ± 2.92[a]	9.47 ± 2.95[a]	21.54 ± 7.15[d]	61.21 ± 4.43[a]	192.71 ± 5.26[b]	3.74 ± 0.44[a]
M♂(119)[2]	10.93 ± 2.16[b]	13.19 ± 3.59[b]	10.94 ± 2.9[b]	7.05 ± 2.87[b]	29.58 ± 8.53[c]	58.47 ± 4.1[b]	198.81 ± 3.58[a]	3.48 ± 0.53[b]

[1]Different letters ([a,b]) indicate highly significant differences in means ($P < 0.05$), and the same letters indicate insignificant differences in means ($P > 0.05$).
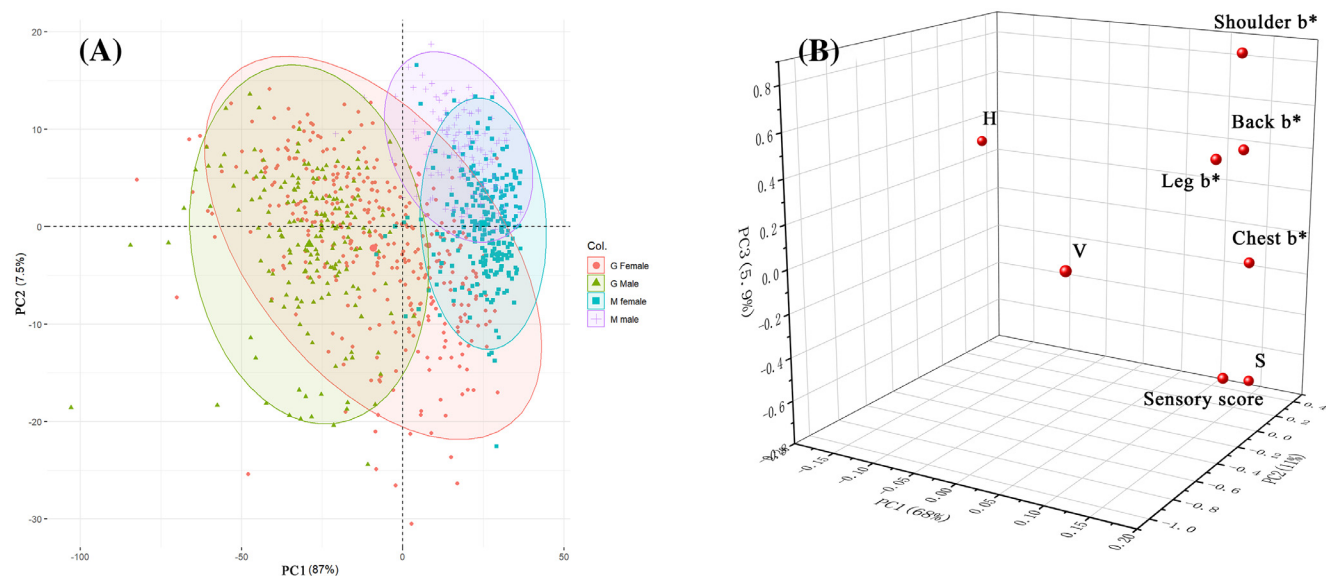[2]The number in parentheses is the number of samples.

Figure 1. Principal component analysis of skin yellowness traits. (A) 2D scatter plot of PCA analysis for each sample; (B) 3D scatter plot of PCA analysis for each skin color trait.

that H and L had different gene expression profiles in duodenal tissue.

To explore the biological functions of the 982 DEGs, GO, and KEGG enrichment analyses were performed on the DEGs. GO enrichment analysis (Figure 2D) showed that DEGs were significantly enriched in transporter activity, tetrapyrrole binding, heme binding, immune system process. The transporter activity pathway is associated with carotenoid absorption. Previous studies have shown that intestinal health is associated with carotenoid absorption, and that chicken skin yellowness may also be regulated by the immune system process, immune response pathway. KEGG enrichment showed that DEGs were significantly enriched in tight junction, steroid hormone biosynthesis, arachidonic acid metabolism, metabolism of xenobiotics by cytochrome P450 pathway (Figure 2F).

Analysis of DEGs Interaction Network and qPCR Validation of Candidate DEGs

In order to explore the interactions of DEGs, we conducted protein interaction analysis of DEGs through STRING website, and the results are shown in Figure 3A. *APOB, ALDH8A1, CYP3A5,* and *CYP2C23*, had high interaction scores, *APOB* has been reported to be associated with carotenoid transport, *ALDH8A1* is involved in retinoid synthesis, and carotenoids can regulate *CYP3A* expression through the pregnane X receptor (**PXR**). To further understand the relationship between DEGs of interest and carotenoid uptake, we generated an interaction network between DEGs and reported yellow skin-related genes using GeneMANIA to show the interaction of DEGs with genes related to skin carotenoid deposition(Figure 3B), which facilitates our better understanding of the relationship between the P450 family, lipid transport, and skin carotenoid deposition. There are physical interactions between *MTTP, APOB* and *ABCG5, CYP1A1* and *SCARB2. MTTP, APOB, SCARB1, APOA1,* and *APOA2* are in the same Pathway (Wu et al., 2010).

To validate the RNA-seq results and to search for genes related to the regulation of chicken skin yellowness, we selected 12 genes underlying lipid transport, P450 family and retrovirus for qPCR validation (Figure 4A), and the trend is consistent with the RNA-seq results (Figure 4B). The primer sequences are shown in Table S1. In addition, we also performed qPCR validation of the carotenoid metabolism-related genes *BMCO1* and *BCO2*, and the carotenoid transporter related gene *SCARB1*. Result showed that they did not differ significantly between H and L (Figure 4C), indicating that the difference in chicken skin yellowness may not be due to the metabolism of carotenoids by *BMCO1* or *BCO2*. The nucleotide blast tool of the National Biotechnology Information Center (**NCBI**) was used to compare and analyze the sequences of *LOC107052719* and *LOC121113436*, and the results showed that their sequences were 99.542% similar to the *Gag* gene of ALVE. (NCBI. Sequence ID: MT263508.1) (Table S8), suggesting the possibility of an endogenous viral influence on carotenoid uptake. The mRNA relative expression levels of these genes were consistent with the results of RNA-seq analysis.
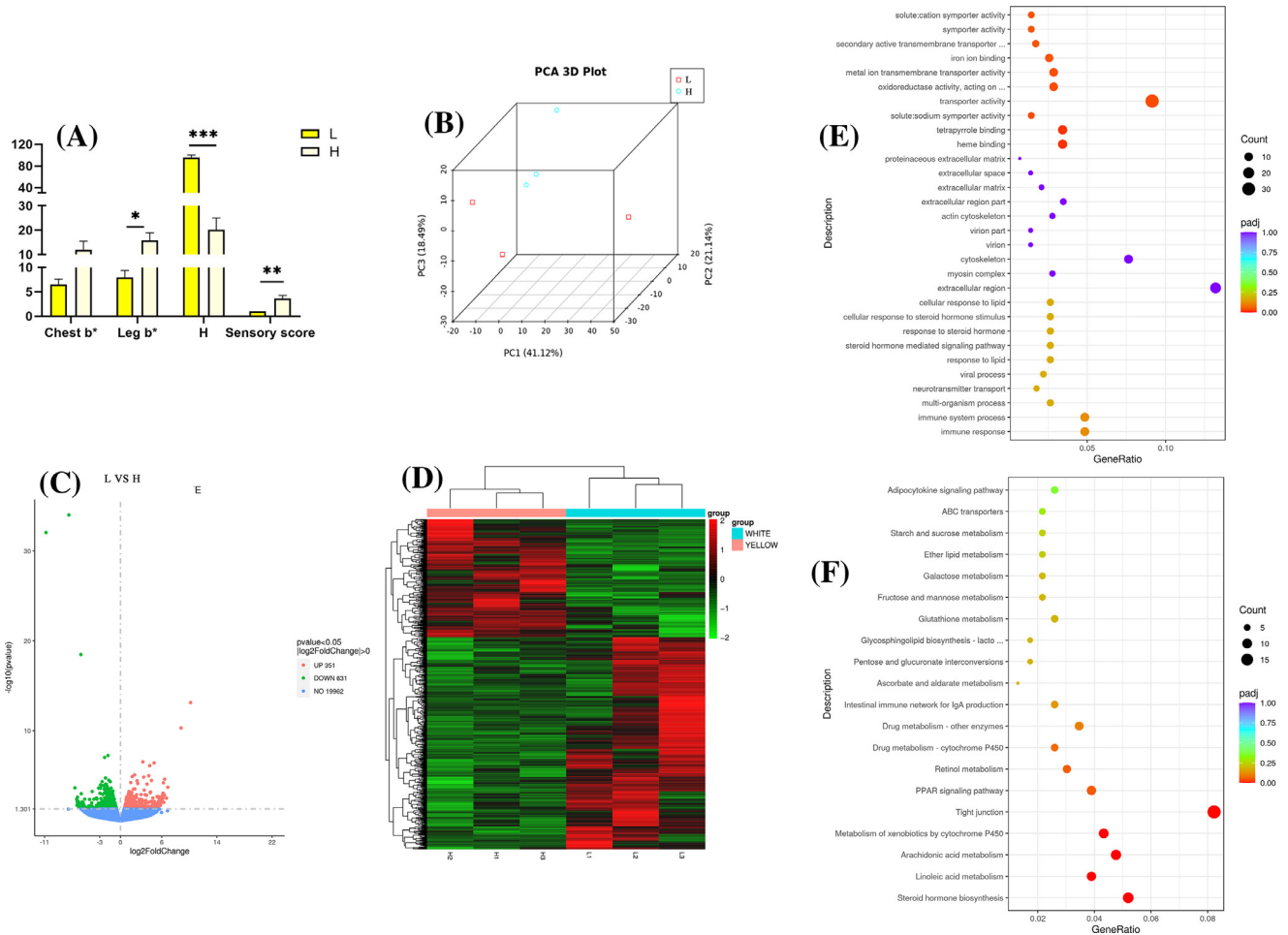
Table. 2. Heritabilities and standard error of skin yellowness traits in G and M lines of chickens.

	G(512)		M(351)	
	h^2	SE(t)	h^2	SE(t)
Chest b*	0.56674	0.09826	0.30567	0.13974
Back b*	0.27693	0.09286	0.07671	0.12797
Shoulder b*	0.24077	0.09269	0.12730	0.11965
Leg b*	0.39521	0.09679	0.24320	0.13745
H	0.58942	0.09651	0.32591	0.14185
S	0.58259	0.09824	0.41077	0.15246
Sensory score	0.48063	0.10007	0.27222	0.14408

Figure 2. Differentiated expressed genes between Line G and Line M Chickens. (A) Skin yellowness traits of RNA-seq samples. *** indicates a significant difference at the level of 0.001, and ** indicates a significant difference at the level of 0.01, and * indicates a significant difference at the level of 0.05; (B) 3D scatter plot of gene expression PCA analysis of RNA-seq samples; (C) the Volcano map of differentially expressed genes; (D) the heat map clusters the FPKM values of the differential genes in each comparison group; (E) KEGG enrichment analysis of DEGs between H and L; (F) GO enrichment analysis of DEGs between H and L. Abbreviations: DEGs, differential expressed genes; GO, Gene Ontology.
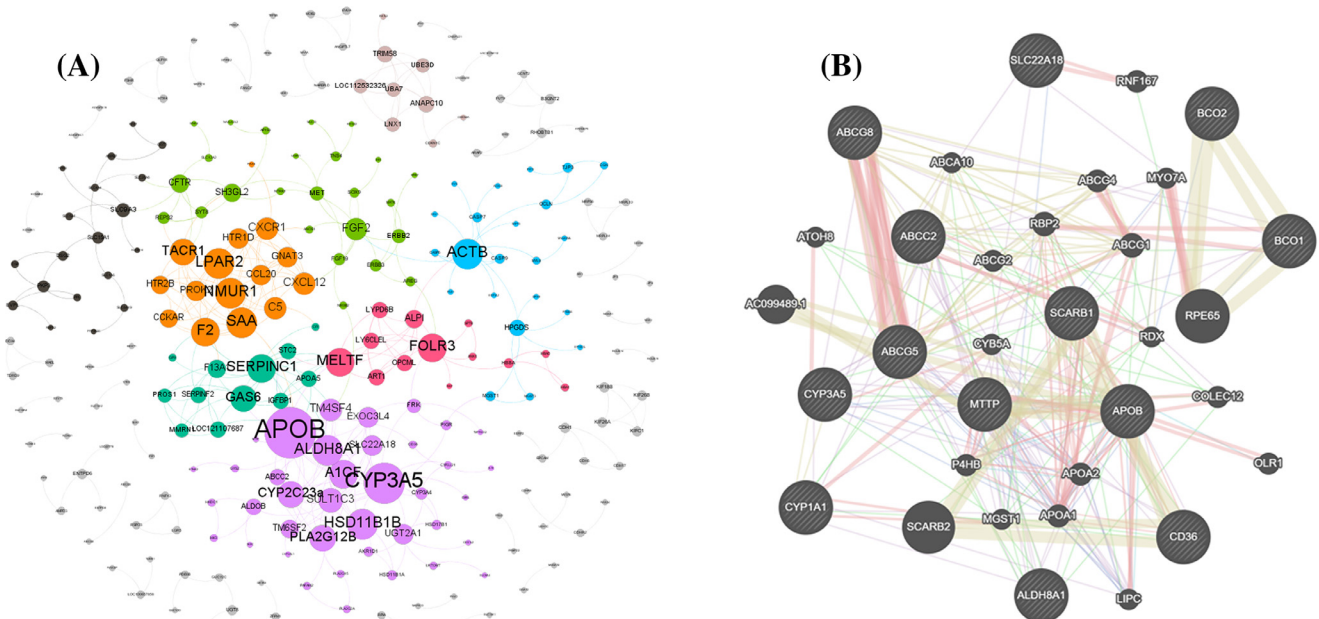

Figure 3. Interaction networks of candidate DEGs that regulate chicken skin yellowness. (A) Protein interaction network of DEGs; (B) protein interaction network of candidate DEGs and genes involved in the regulation of chicken skin yellowness. Abbreviation: DEGs, differential expressed genes.
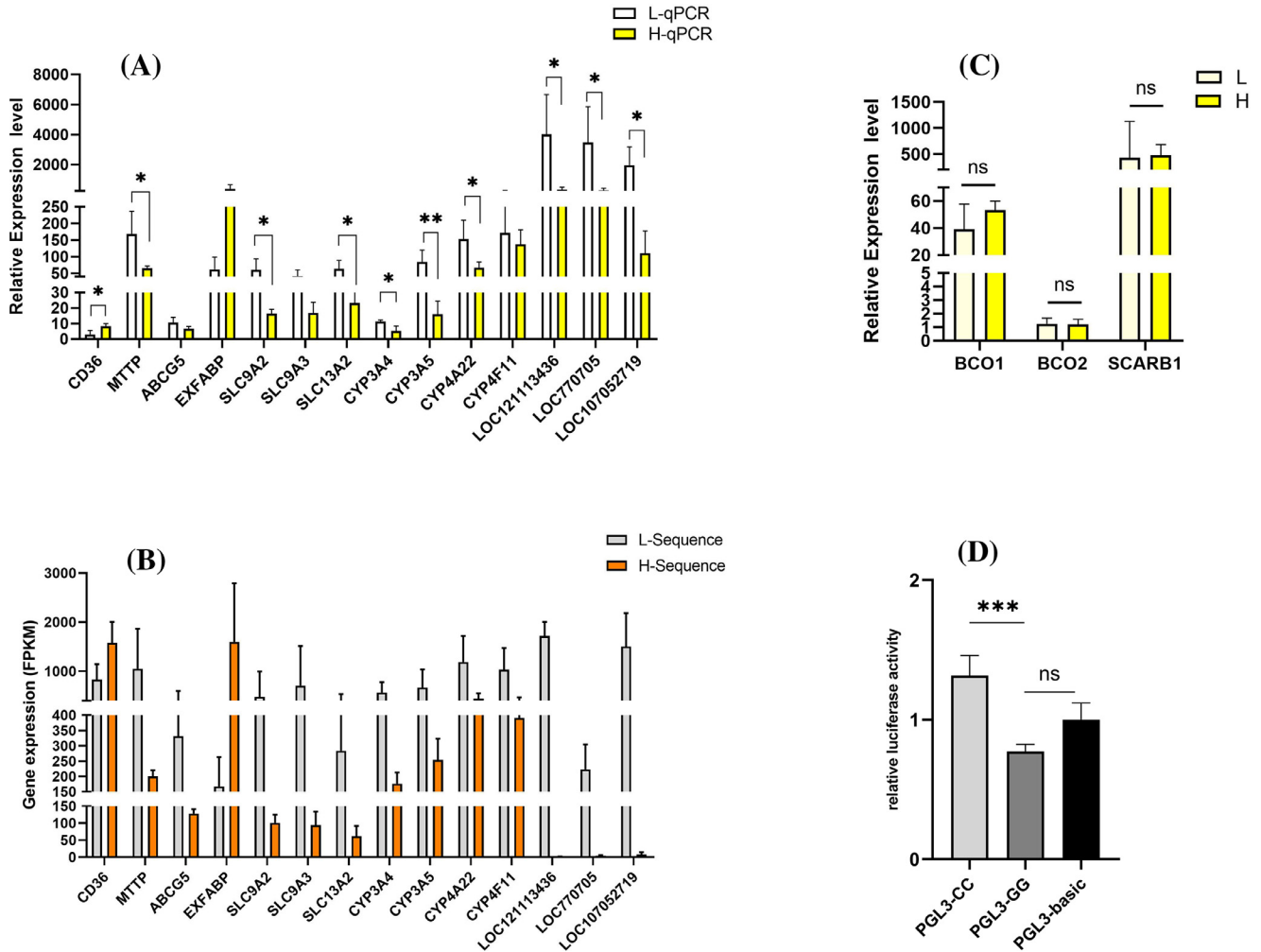
Figure 4. qPCR validation of candidate DEGs and effect of SNP on *CD36* promoter activity. (A) Relative mRNA expression levels of RNA extracted from H and L. ** Indicates a significant difference at the level of 0.01, and * indicates a significant difference at the level of 0.05. (B) FPKM of candidate DEGs. (C) Relative mRNA expression levels of chicken skin yellowness candidate genes in the duodenum. (D) Dual-luciferase assay result for PGL3-CC, PGL3-GG, PGL3-basic(control) transfected LMH cells after 48 h. *** Indicates $P<0.001$. Abbreviations: DEGs, differential expressed genes; SNP, single nucleotide polymorphism.

Identification of SNPs Associated With Chicken Skin Yellowness on CD36

To investigate the markers in the *CD36* gene that could be used for molecular breeding of chicken skin yellowing, we identified SNP variations through amplifying a fragment upstream of the *CD36* gene by PCR with the primer sequences shown in Table S1. DNA fragments from 338 females and 185 males of Line G were sequenced. Three SNPs, g.4429G>C g.4470G>A, g.4478C>G, were identified (Figure S3), of which g.4478C>G (chromosome 1, base 11564048 C>G) was located at 1915 bases of the *CD36* gene and was found to be associated with skin yellowness (Table 3). The g.4478C>G is consistent with Hardy-Weinberg equilibrium, and the CC genotype is a dominant genotype, which belongs to the low polymorphism (Table S4). Chickens with the GG genotype had significantly less yellow skin staining on the chest, back, and legs than those with the CC and CG genotypes, and there were significant differences in photo hue. The g.4478C>G

may be a candidate molecular marker for chicken skin yellowness improvement.

In addition, other 2 SNPs (Figure S3), named g.93C>T (chromosome 1, base 11332036 C>T) and g.149C>G (chromosome 1, base 11332088 C>G) on the 3'UTR of the *CD36* gene, were significantly associated with skin yellowness. Since the gene frequencies of these 2 SNPs were significantly different in the G and M lines (Table S5), the 2 lines were analyzed separately for association analysis (Table S6). Results showed opposite dominant genotypes for g.93C>T and g.149C>G in the G and M lines. TT genotype of g.93C>T and CC genotype of g.149C>G both had higher skin yellowness than other genotypes, which was consistent in the two lines.

SNP affects CD36 Promoter Activity

Prediction of transcription factor binding sites for CC and GG genotype sequences of g.4478C>G by the online tool AliBaba 2.1 (http://gene-regulation.com/pub/

Table 3. Association analysis of *CD36* SNP g.4478C>G with skin yellowness traits (Mean ± SEM).

	CC[1](393)	CG[1](105)	GG[1](25)	*P* value	PVE[2]
Chest b*	9.95 ± 3.04^a	9.71 ± 2.95^a	8.69 ± 2.17^b	0.005	0.073%
Back b*	11.67 ± 4.37^a	10.35 ± 3.39^{ab}	9.72 ± 1.95^b	0.016	0.689%
Shoulder b*	10.89 ± 3.22	11.06 ± 3.12	10.41 ± 2.19	0.113	0.191%
Leg b*	6.81 ± 3.86^a	6.84 ± 4.17^a	5.47 ± 3.21^b	0.023	0.192%
H	45.98 ± 24.41^a	52.51 ± 23.05^a	59.65 ± 17.39^b	0.000	0.024%
S	56.57 ± 7.02	55.84 ± 7.44	54.56 ± 5.58	0.157	3.214%
Sensory score	2.79 ± 1.03^a	2.61 ± 0.95^a	2.36 ± 0.69^b	0.002	0.008%

[1]Different letters ([a,b]) indicate highly significant differences in means ($P < 0.05$), and the same letters indicate insignificant differences in means ($P > 0.05$).

[2]PVE represents the percentage of phenotypic variance explained.

programs/alibaba2/index.html) revealed that the CC genotype has more possible transcription factor binding sites than the GG genotype (Table S7). RAR-alpha and RAR-beta are retinoic acid receptors that regulate gene transcription. Dual-luciferase assay result showed that the promoter activity of the CC genotype was significantly higher than that of the GG genotype (Figure 4D), which may be a contributor to the differential expression of *CD36*.

DISCUSSION

In recent years, many researchers have studied the genetic mechanism of skin yellowness in chickens. *BCO2* was found to be associated with the degradation of carotenoids to colorless derivatives (Amengual et al., 2011), with three SNPs significantly associated with the yellow skin trait(Eriksson et al., 2008), however, they may be able to distinguish between white-skinned and yellow-skinned chickens but not between chickens with high and low skin yellowness (Wu et al., 2021). In addition, it was found that a SNP on *BCO2* was associated with calf skin color traits (Jin et al., 2016). In this study, *BCO2* expression was lower in the duodenum and was not differentially expressed between the high and low yellowness chickens. Therefore, *BCO2* may not function primarily in the duodenum.

Skin deposited carotenoids are mainly obtained from food. The absorption and bioconversion of dietary carotenoids primarily take place in the intestine, where carotenoids form mixed micelles with amphiphilic and hydrophobic compounds including bile salts, cholesterol, fatty acids, monoacylglycerides, and phospholipids (Reboul 2013; von Lintig et al., 2020). *CD36, SLC9A3, SLC13A2, MTTP* and other lipid transport-related genes were differentially expressed in different yellowness chickens, which might affect the absorption of carotenoids in the intestine and thus the skin yellowness. *CD36* and *SCARB1* are key participants in intestinal carotenoid absorption (Moussa et al., 2008; Mapelli-Brahm et al., 2019). Mutations in the *SCARB1* gene change yellow feathers to white feathers in birds by affecting the uptake of carotenoids (Tourkova et al., 2020). In this study, *CD36* is highly expressed in the duodenum of chickens with high skin yellowness, but on the contrary in chickens with low skin yellowness. *CD36* is a scavenger receptor class B protein (SR-B2) that

serves various functions in lipid metabolism and signaling (Glatz et al., 2022). It involved in lycopene, lutein (Moussa et al., 2011) and α-carotene absorption (Borel et al., 2013). A high level of *CD36* expression may mean that the intestinal is more capable of absorbing carotenoids. Therefore, *CD36* is one of the most potential candidates to regulate yellowing of chicken skin.

In *CD36*, several SNP have been found to be associated with the absorption of lutein (Meyers et al., 2014), zeaxanthin (Borel et al., 2011) and β- cryptoxanthin (Borel et al., 2013). We showed that g.4478C>G in the upstream region of *CD36* is significantly associated with chicken skin yellowness. Further transcription factor prediction showed that CC genotype in this SNP position has more RAR transcription factor binding sites than the GG genotype, and RAR has been reported to regulate *CD36* expression (Zhao et al., 2022) and affect fatty acid uptake (Cassim Bawa et al., 2022). The results of dual fluorescein reporter assays in this study further suggested that the CC genotype has higher transcriptional activity than the GG genotype. Chickens with the CC genotype, where the RAR binding site may be present, had a higher degree of yellowing compared to the GG genotype, implying that the high yellowness of the CC genotype was due to a higher level of RAR binding to enhance *CD36* gene expression activity.

KEGG enrichment analysis showed significant enrichment in the cytochrome P450 family, *CYP3A4, CYP3A5*, and the cytochrome P450 pathway was also found to be enriched for differences in yellowness in skin RNA-seq results (Wu et al., 2021), and cytochrome P3A80 has been shown to be a strong candidate for carotenoid ketolase in amphibians (Twomey et al., 2020). *CYP2J19* was found to convert yellow carotenoids to red carotenoids in birds (Kirschel et al., 2020), while birds may convert lutein to zeaxanthin (Crothers et al., 2016). Therefore, cytochrome P450-related DEGs may be candidates for regulating skin yellowness in chickens.

We innovatively investigated chicken skin yellowness trait in terms of intestinal absorption by sequencing the duodenum transcriptome, revealing potential candidate genes and identifying a SNP associated with chicken skin yellowness that could be used for skin yellowness selection. There are physical interactions between *MTTP, APOB* and *ABCG5, CYP1A1* and *SCARB2*. *MTTP, APOB, SCARB1, APOA1,* and *APOA2* are in

the same Pathway (Wu et al., 2010). DEGs are closely related to carotenoid uptake transport. Chicken skin yellowness may be affected by a complex multigene regulatory network and mutations in individual genes may not explain this trait well. This study only sequenced duodenal tissues and attempted to explain the differences in chicken skin yellowness by *CD36*. The effects of other intestinal tracts on chicken skin yellowness and the synergistic effects between DEGs remain to be further investigated.

CONCLUSIONS

In summary, we performed transcriptome sequencing of the duodenum and identified 982 DEGs in chickens with high and low skin yellowness, of which *CD36* was highly expressed in chickens with high skin yellowness and vice versa in chickens with low skin yellowness. We identified a SNP upstream of the *CD36* gene had a significant effect on skin yellowness. All our findings represent a critical step in understanding the genetic basis of skin yellowing in chickens and will help to further unravel the molecular mechanisms of the traits involved.

ACKNOWLEDGMENTS

DISCLOSURES

The authors declare no conflicts of interest.

SUPPLEMENTARY MATERIALS

Supplementary material associated with this article can be found in the online version at doi:10.1016/j.psj.2022.102469.

REFERENCES

Amengual, J., G. P. Lobo, M. Golczak, H. N. Li, T. Klimova, C. L. Hoppel, A. Wyss, K. Palczewski, and J. von Lintig. 2011. A mitochondrial enzyme degrades carotenoids and protects against oxidative stress. FASEB J 25:948–959.

Bhosale, P., A. J. Larson, J. M. Frederick, K. Southwick, C. D. Thulin, and P. S. Bernstein. 2004. Identification and characterization of a Pi isoform of glutathione S-transferase (GSTP1) as a zeaxanthin-binding protein in the macula of the human eye. J. Biol. Chem. 279:49447–49454.

Borel, P., F. S. de Edelenyi, S. Vincent-Baudry, C. Malezet-Desmoulin, A. Margotat, B. Lyan, J. M. Gorrand, N. Meunier, S. Drouault-Holowacz, and S. Bieuvelet. 2011. Genetic variants in BCMO1 and CD36 are associated with plasma lutein concentrations and macular pigment optical density in humans. Ann. Med. 43:47–59.

Borel, P., G. Lietz, A. Goncalves, F. S. de Edelenyi, S. Lecompte, P. Curtis, L. Goumidi, M. J. Caslake, E. A. Miles, C. Packard, P. C. Calder, J. C. Mathers, A. M. Minihane, F. Tourniaire, E. Kesse-Guyot, P. Galan, S. Hercberg, C. Breidenassel, M. G. Gross, M. Moussa, A. Meirhaeghe, and E. Reboul. 2013. CD36 and SR-BI are involved in cellular uptake of provitamin A carotenoids by Caco-2 and HEK cells, and some of their genetic variants are associated with plasma concentrations of these micronutrients in humans. J. Nutr. 143:448–456.

Budny, J. A. 2015. Encyclopedia of toxicology, 3rd edition. Int. J. Toxicol 34:366–367.

Cassim Bawa, F. N., Y. Xu, R. Gopoju, N. M. Plonski, A. Shiyab, S. Hu, S. Chen, Y. Zhu, K. Jadhav, T. Kasumov, and Y. Zhang. 2022. Hepatic retinoic acid receptor alpha mediates all-trans retinoic acid's effect on diet-induced hepatosteatosis. Hepatol. Commun 6:2665–2675.

Crothers, L., R. A. Saporito, J. Yeager, K. Lynch, C. Friesen, C. L. Richards-Zawacki, K. McGraw, and M. Cummings. 2016. Warning signal properties covary with toxicity but not testosterone or aggregate carotenoids in a poison frog. Evol. Ecol. 30:601–621.

During, A., S. Doraiswamy, and E. H. Harrison. 2008. Xanthophylls are preferentially taken up compared with beta-carotene by retinal cells via a SRBI-dependent mechanism. J. Lipid Res. 49:1715–1724.

Eriksson, J., G. Larson, U. Gunnarsson, B. Bed'hom, M. Tixier-Boichard, L. Stromstedt, D. Wright, A. Jungerius, A. Vereijken, E. Randi, P. Jensen, and L. Andersson. 2008. Identification of the Yellow skin gene reveals a hybrid origin of the domestic chicken. PLoS Genet 4:1–8.

Glatz, J. F. C., M. Nabben, and J. Luiken. 2022. CD36 (SR-B2) as master regulator of cellular fatty acid homeostasis. Curr. Opin. Lipidol. 33:103–111.

Jin, S., J. H. Lee, D. W. Seo, M. Cahyadi, N. R. Choi, K. N. Heo, C. Jo, and H. B. Park. 2016. A major locus for quantitatively measured shank skin color traits in Korean native chicken. Asian-Australas. J. Anim. Sci. 29:1555–1561.

Kirschel, A. N. G., E. C. Nwankwo, D. K. Pierce, S. M. Lukhele, M. Moysi, B. O. Ogolowa, S. C. Hayes, A. Monadjem, and A. Brelsford. 2020. CYP2J19 mediates carotenoid colour introgression across a natural avian hybrid zone. Mol. Ecol. 29:4970–4984.

Krieger, M. 1999. Charting the fate of the "good cholesterol": identification and characterization of the high-density lipoprotein receptor SR-BI. Annu. Rev. Biochem 68:523–558.

Langi, P., S. Kiokias, T. Varzakas, and C. Proestos. 2018. Carotenoids: from plants to food and feed industries. Methods Mol. Biol 1852:57–71.

Littlefield, L. H., J. K. Bletner, H. V. Shirley, and O. E. Goff. 1972. Locating the site of absorption of xanthophylls in the chicken by a surgical technique. Poult. Sci. 51:1721–1725.

Londos, C., J. Gruia-Gray, D. L. Brasaemle, C. M. Rondinone, T. Takeda, N. K. Dwyer, T. Barber, A. R. Kimmel, and E. J. Blanchette-Mackie. 1996. Perilipin: possible roles in structure and metabolism of intracellular neutral lipids in adipocytes and steroidogenic cells. Int. J. Obes. Relat. Metab. Disord 20(Suppl 3) S97-101.

Mapelli-Brahm, P., M. Margier, C. Desmarchelier, C. Halimi, M. Nowicki, P. Borel, A. J. Melendez-Martinez, and E. Reboul. 2019. Comparison of the bioavailability and intestinal absorption sites of phytoene, phytofluene, lycopene and beta-carotene. Food Chem 300:125232.

McLean, J. A., F. Karadas, P. F. Surai, R. M. McDevitt, and B. K. Speake. 2005. Lipid-soluble and water-soluble antioxidant activities of the avian intestinal mucosa at different sites along the intestinal tract. Comp. Biochem. Physiol. B Biochem. Mol. Biol. 141:366–372.

Meyers, K. J., J. A. Mares, R. P. Igo Jr., B. Truitt, Z. Liu, A. E. Millen, M. Klein, E. J. Johnson, C. D. Engelman, C. K. Karki, B. Blodi, K. Gehrs, L. Tinker, R. Wallace, J. Robinson, E. S. LeBlanc, G. Sarto, P. S. Bernstein, J. P. SanGiovanni, and S. K. Iyengar. 2014. Genetic evidence for role of carotenoids in age-related macular degeneration in the carotenoids in age-related eye disease study (CAREDS). Invest. Ophthalmol. Vis. Sci. 55:587–599.

Moussa, M., E. Gouranton, B. Gleize, C. El Yazidi, I. Niot, P. Besnard, P. Borel, and J. F. Landrier. 2011. CD36 is involved in lycopene and lutein uptake by adipocytes and adipose tissue cultures. Mol. Nutr. Food Res. 55:578–584.

Moussa, M., J. F. Landrier, E. Reboul, O. Ghiringhelli, C. Comera, X. Collet, K. Frohlich, V. Bohm, and P. Borel. 2008. Lycopene absorption in human intestinal cells and in mice involves scavenger receptor class B type I but not Niemann-Pick C1-like 1. J. Nutr. 138:1432–1436.

Phan, C. T., and P. Tso. 2001. Intestinal lipid absorption and transport. Front. Biosci. 6:D299–D319.

Phelan, D., A. Prado-Cabrero, and J. M. Nolan. 2018. Analysis of lutein, zeaxanthin, and meso-zeaxanthin in the organs of carotenoid-supplemented chickens. Foods 7:1–8.

Reboul, E. 2013. Absorption of vitamin A and carotenoids by the enterocyte: focus on transport proteins. Nutrients 5:3563–3581.

Ren, T., W. Li, D. Liu, K. Liang, X. Wang, H. Li, R. Jiang, Y. Tian, X. Kang, and Z. Li. 2019. Two insertion/deletion variants in the promoter region of the QPCTL gene are significantly associated with body weight and carcass traits in chickens. Anim. Genet. 50:279–282.

Sakudoh, T., T. Iizuka, J. Narukawa, H. Sezutsu, I. Kobayashi, S. Kuwazaki, Y. Banno, A. Kitamura, H. Sugiyama, N. Takada, H. Fujimoto, K. Kadono-Okuda, K. Mita, T. Tamura, K. Yamamoto, and K. Tsuchida. 2010. A CD36-related transmembrane protein is coordinated with an intracellular lipid-binding protein in selective carotenoid transport for cocoon coloration. J. Biol. Chem. 285:7739–7751.

Soccio, R. E., and J. L. Breslow. 2003. StAR-related lipid transfer (START) proteins: mediators of intracellular lipid metabolism. J. Biol. Chem. 278:22183–22186.

Tabunoki, H., S. Higurashi, O. Ninagi, H. Fujii, Y. Banno, M. Nozaki, M. Kitajima, N. Miura, S. Atsumi, K. Tsuchida, H. Maekawa, and R. Sato. 2004. A carotenoid-binding protein (CBP) plays a crucial role in cocoon pigmentation of silkworm (Bombyx mori) larvae. FEBS Lett 567:175–178.

Tourkova, I. L., S. F. Dobrowolski, C. Secunda, M. Zaidi, I. Papadimitriou-Olivgeri, D. J. Papachristou, and H. C. Blair. 2020. The high-density lipoprotein receptor Scarb1 is required for normal bone differentiation in vivo and in vitro (vol 124, pg 564, 2020). Lab. Invest. 100:790–794.

Tuzcu, M., C. Orhan, O. E. Muz, N. Sahin, V. Juturu, and K. Sahin. 2017. Lutein and zeaxanthin isomers modulates lipid metabolism and the inflammatory state of retina in obesity-induced high-fat diet rodent model. BMC Ophthalmol 17:1–9.

Twomey, E., J. D. Johnson, S. Castroviejo-Fisher, and I. Van Bocxlaer. 2020. A ketocarotenoid-based colour polymorphism in the Sira poison frog Ranitomeya sirensis indicates novel gene interactions underlying aposematic signal variation. Mol. Ecol. 29:2004–2015.

Tyczkowski, J. K., and P. B. Hamilton. 1986. Absorption, transport, and deposition in chickens of lutein diester, a carotenoid extracted from marigold (Tagetes erecta) petals. Poult Sci 65:1526–1531.

Vage, D. I., and I. A. Boman. 2010. A nonsense mutation in the beta-carotene oxygenase 2 (BCO2) gene is tightly associated with accumulation of carotenoids in adipose tissue in sheep (Ovis aries). BMC Genet 11:1–6.

van Bennekum, A., M. Werder, S. T. Thuahnai, C. H. Han, P. Duong, D. L. Williams, P. Wettstein, G. Schulthess, M. C. Phillips, and H. Hauser. 2005. Class B scavenger receptor-mediated intestinal absorption of dietary beta-carotene and cholesterol. Biochemistry 44:4517–4525.

von Lintig, J., J. Moon, J. Lee, and S. Ramkumar. 2020. Carotenoid metabolism at the intestinal barrier. Biochim. Biophys. Acta Mol. Cell Biol. Lipids 1865:158580.

von Lintig, J., and K. Vogt. 2000. Filling the gap in vitamin A research. Molecular identification of an enzyme cleaving beta-carotene to retinal. J. Biol. Chem 275:11915–11920.

Wu, G. M., X. Feng, and L. Stein. 2010. A human functional protein interaction network and its application to cancer data analysis. Genome Biol 11:R53.

Wu, J., Z. Lin, G. Chen, Q. Luo, Q. Nie, X. Zhang, and W. Luo. 2021. Characterization of chicken skin yellowness and exploration of genes involved in skin yellowness deposition in chicken. Front. Physiol. 12:585089.

Zhao, Z., Z. T. Deng, S. Huang, M. Ning, Y. Feng, Y. Shen, Q. S. Zhao, and Y. Leng. 2022. Alisol B alleviates hepatocyte lipid accumulation and lipotoxicity via regulating RARalpha-PPAR-gamma-CD36 cascade and attenuates non-alcoholic steatohepatitis in mice. Nutrients 14:2411.